

First order character and observable signatures of topological quantum phase transitions

A. Amaricci¹, J. C. Budich^{2,3}, M. Capone¹, B. Trauzettel⁴, and G. Sangiovanni⁴

¹*Democritos National Simulation Center, Consiglio Nazionale delle Ricerche, Istituto Officina dei Materiali (IOM) and Scuola Internazionale Superiore di Studi Avanzati (SISSA), Via Bonomea 265, 34136 Trieste, Italy*

²*Institute for Theoretical Physics, University of Innsbruck, 6020 Innsbruck, Austria*

³*Institute for Quantum Optics and Quantum Information, Austrian Academy of Sciences, 6020 Innsbruck, Austria and*

⁴*Institut für Theoretische Physik und Astrophysik, Universität Würzburg, Am Hubland, D-97074 Würzburg, Germany*

(Dated: December 7, 2024)

Topological quantum phase transitions are characterised by changes in global topological invariants. These invariants classify many body systems beyond the conventional paradigm of local order parameters describing spontaneous symmetry breaking. For non-interacting electrons, it is well understood that such transitions are continuous and always accompanied by a gap-closing in the energy spectrum, given that the symmetries protecting the topological phase are maintained. Here, we demonstrate that sufficiently strong electron-electron interaction can fundamentally change the situation: we discover a topological quantum phase transition of first order character in the genuine thermodynamic sense, that occurs without gap closing. Our theoretical study reveals the existence of a quantum critical endpoint associated with an orbital instability on the transition line between a 2D topological insulator and a trivial band insulator. Remarkably, this phenomenon entails unambiguous signatures associated to the orbital occupations that can be detected experimentally.

INTRODUCTION

The advent of topological insulators [1–3] has given a surprising twist to the venerable topic of band structure physics: Triggered by the theoretical prediction [4–6] and experimental observation [7] of the quantum spin Hall effect, topological aspects of band insulators and superconductors have become one of the most active research fields in physics, culminating in the discovery of a new periodic table [8–10] that exhaustively lists all topologically distinct band structures in the ten Altland-Zirnbauer symmetry classes [11]. For the integer quantum Hall effect, the archetype of a topological state, the experimental discovery of the striking quantisation of a natural response quantity, namely the Hall conductance [12], preceded its theoretical explanation [13, 14] in terms of topology. In contrast, most of the topological invariants occurring in the periodic table of topological states are not directly related to bulk observable quantities. The identification of further experimental fingerprints is hence a key challenge in our physical understanding of topological phases.

Beyond the independent-particle approximation, new scenarios may arise in strongly correlated systems, due to the interplay between spin, charge and orbital degrees of freedom. Along these lines, systems where the band structure topology is induced by electron-electron interaction have been reported [15–23]. Yet, a natural and still open question is whether correlation-induced topological insulators can exhibit experimental signatures, which enable an unambiguous distinction from their weakly correlated counterparts. The focus of our present study is on the identification of such experimentally accessible finger-

prints in correlation-driven topological quantum phase transitions (TQPTs) that take place before the onset of long-range order.

For non-interacting electrons, TQPTs are always continuous and accompanied by the closure of the single-particle energy gap, given that the symmetries protecting the topological phase are preserved. Here, we report for the first time the occurrence of a *first order* TQPT from a trivial time reversal symmetric band insulator (BI) to a strongly correlated quantum spin Hall insulator (QSHI) in a microscopic model. We reveal the thermodynamic nature of this transition and demonstrate that it is associated with observable signatures reflecting genuine correlation effects. To this end, we solve a two-orbital Hubbard model with Dynamical Mean-Field Theory (DMFT), showing that the BI to QSHI transition takes place without the continuous closing of the band gap in the electronic spectrum if the Coulomb repulsion is large enough. In this strongly-correlated regime, the interaction-induced QSHI is thus in proximity to a first order transition line that is separated from the continuous transition by a quantum critical endpoint in the Landau-Ginzburg sense of thermodynamics. As a consequence, in contrast to the uncorrelated case, the topologically trivial and non-trivial states existing on opposite sides of the first order line become distinguishable not only in a formal topological, but also in a practical thermodynamic sense. As we demonstrate below, the microscopic mechanism inducing this phenomenology is a correlation-driven criticality in the orbital channel. A direct, yet crucial, implication of this result is the natural identification of a critical behaviour in simple measurable

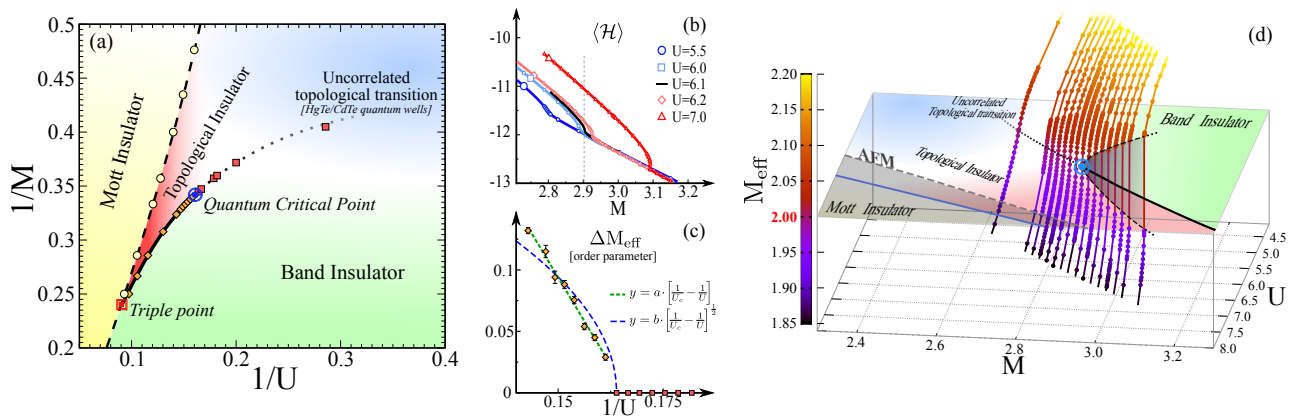


Figure 1. DMFT results for the two-band Hubbard model, defined by the Hamiltonian (1), for $T = 0$, $\lambda = 0.3$ and $J = U/4$. (a) Phase-diagram as a function of the inverse interaction strength $1/U$ and the inverse Dirac mass $1/M$. The topological transition line (dotted black line and red squares) starts from the upper right corner, where conventional uncorrelated semiconductors are situated, and bends down towards the triple point (bigger red square) in the bottom left corner. A quantum critical point at $(1/U_c, 1/M_c)$ (bigger blue circle), associated to critical behaviour in the orbital channel, divides the topological transition line in two parts. The one (solid black lines and orange diamonds) bordering on the red wedge representing the non-trivial insulator, corresponds to a first order phase transition. The Mott insulating region (yellow) is found for small values of $1/U$, whereas the trivial BI exists at large $1/U$, in the green bottom right corner. (b) Total energy $\langle \mathcal{H} \rangle$ as a function of M , for fixed values of U . The slope of $\langle \mathcal{H} \rangle$ displays a discontinuity for $U > U_c = 6.1$, demonstrating the thermodynamic first-order character of the transition. (c) $\Delta M_{\text{eff}} = M_{\text{eff}}(\text{BI}) - M_{\text{eff}}(\text{QSHI})$ along the whole topological transition line, estimated via a linear extrapolation of the data of panel (d) across the discontinuity. Our current numerical accuracy allows us to determine that a β critical exponent of 1 (green dashed line), characteristic of a mean-field Gross-Neveu universality class [24], gives a better description of ΔM_{eff} than a Ising-like $\beta = 1/2$ (blue dashed line). (d) Behaviour of the effective mass M_{eff} in the proximity of the quantum critical point. The horizontal plane at $M_{\text{eff}} = 2$ separates the non-trivial phase with $M_{\text{eff}} < 2$ from the trivial one. The critical point (marked here by the big blue circle, as in Fig. 1a) is the endpoint of the smooth topological transition and beyond it, i.e. along the solid black line, a first order jump in M_{eff} between the BI and the QSHI occurs. An antiferromagnetic phase sets in at larger U (dashed line), away from the critical point.

quantities related to the orbital polarisation.

MODEL

We study a minimal two band Fermi-Hubbard model with both inter- and intra-band interactions on a two-dimensional (2D) square lattice exhibiting the quantum spin Hall effect [25]. The model Hamiltonian reads as

$$\mathcal{H} = \sum_{\mathbf{k}} \psi_{\mathbf{k}}^{\dagger} \hat{\mathbf{H}}_0(\mathbf{k}) \psi_{\mathbf{k}} + \sum_i \mathcal{H}_{\text{int}}(i),$$

$$\mathcal{H}_{\text{int}}(i) = (U - J) \frac{N_i(N_i - 1)}{2} - J \left(\frac{N_i^2}{4} + S_{zi}^2 - 2T_{zi}^2 \right) \quad (1)$$

where $\psi_{\mathbf{k}} = (c_{1\mathbf{k}\uparrow} \ c_{2\mathbf{k}\uparrow} \ c_{1\mathbf{k}\downarrow} \ c_{2\mathbf{k}\downarrow})$ and the operator $c_{\mathbf{k}\alpha\sigma}^{\dagger}$ ($c_{\mathbf{k}\alpha\sigma}$) creates (annihilates) an electron in orbital $\alpha = 1, 2$ with momentum \mathbf{k} and spin σ . N_i is the number operator for the electrons on site i , summed over α and σ . S_{zi} and T_{zi} are the z -components of the total spin and orbital pseudo-spin, respectively. When referring to the local components of these operators, we will drop the subscript i . The local orbital polarisation, e.g., will therefore read $T_z = (n_{1\uparrow} + n_{1\downarrow} - n_{2\uparrow} - n_{2\downarrow})/2 = (n_1 - n_2)/2$.

The non-interacting part $\hat{\mathbf{H}}_0$ of the Hamiltonian (1) conserves S_z , i.e., it has a $U(1)$ spin rotation symmetry and, hence, is block diagonal in spin: $\hat{\mathbf{H}}_0(\mathbf{k}) = \text{Diag}[\hat{h}(\mathbf{k}), \hat{h}^*(-\mathbf{k})]$. The relation between the two blocks is imposed by time reversal symmetry (TRS). Denoting the orbital pseudo-spin by τ , the individual blocks have the form $\hat{h}(\mathbf{k}) = d_{\mathbf{k}}^i \tau_i$, with $d_{\mathbf{k}}^x = \lambda \sin(k_x)$, $d_{\mathbf{k}}^y = \lambda \sin(k_y)$, $d_{\mathbf{k}}^z = M - \cos(k_x) - \cos(k_y)$, describing a system of two bands of width $W = 4$ in our units of energy, separated by an energy splitting $2M$ and coupled with a nonzero inter-orbital hybridisation λ . The value of λ has been fixed to 0.3 and we have checked that our results are qualitatively robust against this choice. We consider an average density of two electrons per site (half-filling), which corresponds to setting the chemical potential μ at the centre of the gap.

In the absence of electron-electron interaction and with the interpretation of $\alpha = 1, 2$ as an electron-like and a hole-like orbital in a semiconductor quantum well, a similar model has been originally introduced [6] for HgTe-CdTe heterostructures where the quantum spin Hall effect has first been experimentally observed [7]. In our model the two orbitals should be regarded as localised electron wave functions of strongly correlated systems or as lowest Wannier functions in a deep optical lattice with

fermionic atoms.

The second term \mathcal{H}_{int} in the Hamiltonian (1) describes the screened local Coulomb repulsion experienced by the fermions, in one of the standard parametrisation [26]. Studies of multi-orbital correlated materials have demonstrated the importance of considering *inter-* and *intra-*orbital Hubbard- U terms as well as the Hund's coupling J , in order to account for the natural tendency of the interacting electrons to maximise S_z and minimise T_z (high-spin configuration) [26].

A non-perturbative solution of our interacting model (1) in the thermodynamic limit is attainable by means of DMFT (see Ref. [27] for a review). This approximation goes beyond the static mean-field (Hartree-Fock) level because it treats the self-energy, which describes all interaction effects entering the single-particle Greens function, as a frequency dependent, though purely local, quantity. The orbital structure, crucial to describe many-body effects on topology [28], is also fully described within DMFT. Here, the self-energy in the orbital pseudo-spin space has the form $\hat{\Sigma}(\omega) = \Sigma(\omega)\tau_z$, where $\Sigma(\omega)$ is a scalar (complex-valued) function. The real part of $\hat{\Sigma}$ at $\omega=0$ renormalises the energy splitting between the two orbitals: $2M_{\text{eff}} = 2M + \text{Tr}[\tau_z \hat{\Sigma}(\omega=0)]$. If J is a nonzero fraction of U , the self-energy correction to $2M$ can be made negative upon increasing U , i.e. the multi-orbital electronic interaction contributes to *reduce* the energy separation between the two orbital bands [29].

DMFT accurately describes three-dimensional transition-metal oxides or partially filled d - or f -electron systems [30–32]. Metal-insulator transitions in two dimensions are treated less accurately, at least from a quantitative perspective, with significant overestimates of the critical temperatures. In this work, however, we deal with insulating phases only and we expect the drawbacks of the local approximation of the self-energy to be less severe. Nevertheless, the method has an intrinsic mean-field character as far as the spatial degrees of freedom are concerned. Therefore any phase transition must have classical critical indexes within the correct universality class.

PHASE DIAGRAM

The zero temperature paramagnetic phase diagram of our model (1) for $\lambda = 0.3$ is shown in Fig. 1(a) in the $1/M$ vs $1/U$ plane. In the $U = 0$ non-interacting limit ($1/U \rightarrow \infty$) we recover the conventional topological transition where the band gap (of size $2M - 4$) closes. This happens at $M = 2$, the point in which a semi-metallic solution separates the trivial BI from the QSHI. At finite U and J , the transition line is defined as $M_{\text{eff}} = 2$ and is marked, in Fig. 1(a), by the dotted and solid black curves going through the red squares and the orange diamonds. Along this line, the topological \mathbb{Z}_2 -invariant, calculated

via the DMFT single-particle Green's function following Refs. [33, 34], changes from 0 in the BI, to 1 in the QSHI.

Our central finding is the existence of a dramatic difference between small and large values of U in the way the topological transition occurs. Along the dotted part of the $M_{\text{eff}} = 2$ line, the transition is qualitatively similar to the non-interacting case [5]: the solution of the model is semi-metallic, i.e. it has no spectral gap but vanishing spectral weight at the Fermi level. For small variations of $1/M$ and/or $1/U$ this semi-metallic state evolves continuously into a fully gapped insulator on both sides, as shown by the leftmost M_{eff} curves of Fig. 1(d). Upon increasing U , the continuous transition line ends at a QCP (marked by a blue point in Fig. 1(a)). Beyond the QCP located at $(1/U_c, 1/M_c)$, the topological transition is no longer accompanied by a semi-metallic solution. This is reflected in the evolution of M_{eff} as a function of M upon approaching the red region of large U in Fig. 1(d): the slope of the curve diverges at the QCP and, after, M_{eff} jumps from a “left” to a “right” value. The size of this discontinuity increases upon increasing U , as indicated by the dashed lines, drawn as guide to the eye.

The topological transition in the correlated part of the phase diagram becomes, therefore, of first order in the usual thermodynamic sense, as also demonstrated by the behaviour of the total energy $\langle \mathcal{H} \rangle$ in Fig. 1(b). For $U < U_c$ both $\langle \mathcal{H} \rangle$ and its first derivative are smooth functions of M , in the range of M shown. For $U = U_c$, $\langle \mathcal{H} \rangle$ develops a discontinuity of the second derivative and, for $U > U_c$, the first derivative of $\langle \mathcal{H} \rangle$ is discontinuous. The difference between M_{eff} in the trivial and in the non-trivial solutions, i.e. ΔM_{eff} computed along the transition line behaves like an order parameter as a function of $1/U$, as shown in Fig. 1(c).

The novel quantum phase transition unveiled by our DMFT calculation cannot be captured by a Hartree-Fock decoupling, for any of the interaction values that we have considered. The critical behaviour of the system at the QCP in the orbital channel is indeed a genuine many-body effect beyond perturbation theory, in line with what was observed for related models in Refs. [35, 36]. Our current numerical accuracy is not good enough for a quantitative prediction of the critical exponents. We however notice that a linear scaling law gives a better fit of ΔM_{eff} than a mean-field Ising-like square root behaviour (see Fig. 1(c)), hinting at a quantum criticality of the mean-field Gross-Neveu universality class [24].

Since this interesting critical behaviour occurs for large interaction, a natural question is whether the onset of antiferromagnetic ordering may obliterate it. Releasing the paramagnetic constraint in our DMFT calculation, we obtain that antiferromagnetism is only stable in the dashed grey area of Fig. 1(d), therefore it does not hide the QCP.

ABSENCE OF GAP CLOSING AND OTHER OBSERVABLE SIGNATURES

Continuous TQPTs associated with gap-closing Dirac cones have been extensively discussed in the recent literature (see Ref. [3, 20] for reviews). Within the independent particle approximation, the topology of topological insulators can only change via such a spectral gap closing if the underlying symmetries of the system are maintained. In contrast, by explicit breaking of TRS [3, 20, 37, 38] or particle number conservation [39], a QSHI can be continuously connected to a trivial band insulator without a gap closing. In the presence of interactions, the single-particle Green's function can acquire zeros that are also associated with changes in the topological invariants [40].

Remarkably, the TQPT line for $U > U_c$ discovered in this work does not fit into any of the above pictures. The topological transition line (solid black curve in Fig. 1(a)) is of first order and is accompanied by a discontinuity – in the sense of a finite jump – in the single-particle Green's function, in particular in the effective Dirac mass parameter M_{eff} (see Fig. 1(c)). We stress that both TRS and particle number conservation are maintained here.

The absence of a gap closing is demonstrated in Fig. 2, in which we compare the evolution of the spectral gap around the Γ -point $\mathbf{k} = 0$ as a function of M for a BI-QSHI transition at $U = 5.5 < U_c$ and at $U = 7.0 > U_c$, respectively. While a gap closing (Dirac cone at the Γ -point) occurs for $U = 5.5$, a finite spectral gap is maintained for $U = 7.0$. In the latter case, indeed, the ground state discontinuously jumps from a gapped BI to a gapped QSHI at the first order transition point.

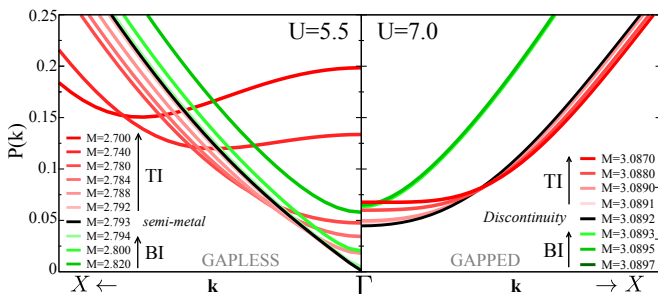


Figure 2. Poles $P(\mathbf{k})$ of the single-particle Green's function near the Γ point $\mathbf{k} = 0$ for $U = 5.5$ (left panel) and $U = 7.0$ (right panel). Since the poles are symmetric with respect to $P(\mathbf{k}) = 0$, we show only the positive ones. The colour coded plots illustrate the modification to the band-structure as the value of M is tuned through the BI-QSHI transition. In the weak interaction regime (left) the transition occurs with a closure of the band-gap giving rise to a semi-metallic state with a Dirac-cone dispersion. For strong interaction (right) the transition takes place without closure of the spectral gap.

The lack of the zero-gap semi-metallic state in the *bulk* electronic structure, illustrated in Fig. 2, is a striking dissimilarity between conventional (continuous) and correlation-driven first order topological transitions. This property is, in principle, also directly measurable in photoemission experiments. Yet, the thermodynamic characterisation of the phase transition that we have unveiled here, allows us to make an even more important step forward in the identification of experimentally detectable differences between trivial and non-trivial phase. We indeed predict discontinuities not only in the spectral gap, but also in other simple physical observables, such as the electronic occupations or the local spin susceptibility, when entering the QSHI at $U > U_c$. This is in stark contrast with topological transitions in weakly correlated systems, which show smooth behaviours of these quantities.

Since the QCP discovered here is associated with a critical behaviour of M_{eff} , it has a direct influence on the orbital polarisation. In Fig. 3(a), we show how $\langle T_z \rangle$ changes from a continuous dependence as a function of M , at small U , to a critical one (infinite slope) at U_c . Eventually, it displays a first order jump beyond the QCP. We can quantify this behaviour by looking at the orbital compressibility

$$\kappa = -2 \frac{\partial \langle T_z \rangle}{\partial M} = -2 \frac{\partial \langle n_1 \rangle}{\partial M}. \quad (2)$$

In Fig. 3(b) we show this quantity as a function of M , for different values of U , before, at and after the QCP. κ displays a maximum at the topological transition, which gets sharper upon increasing U and eventually diverges at the QCP. For $U > U_c$ both the “left” and the “right” value of the orbital compressibility across the first order jump are finite again and decrease with U . Since the orbital-resolved occupations can be measured by, e.g., resonant orbital reflectometry [41, 42], the divergence of the orbital compressibility is an ideal experimental marker of the interaction-driven topological transition, as well as of the thermodynamic distinction between BI and QSHI, discussed here.

In addition to the orbital occupations, we can identify specific signatures of interaction-induced topological phase transition connected to the spin degrees of freedom too. Unlike conventional band insulators, Mott systems are characterised by the presence of (instantaneous) local magnetic moments and by a Curie-like ($\propto 1/T$) local spin susceptibility. The latter is defined as

$$\chi_{\text{loc}} = \int_0^{1/T} d\tau \langle T_\tau S_z(\tau) S_z(0) \rangle. \quad (3)$$

Information on the magnetic moments and on χ_{loc} can be gained in neutron scattering experiments as well as in nuclear magnetic resonance experiments through the Knight shift [43, 44]. The instantaneous square local moment calculated within DMFT (not shown) behaves very

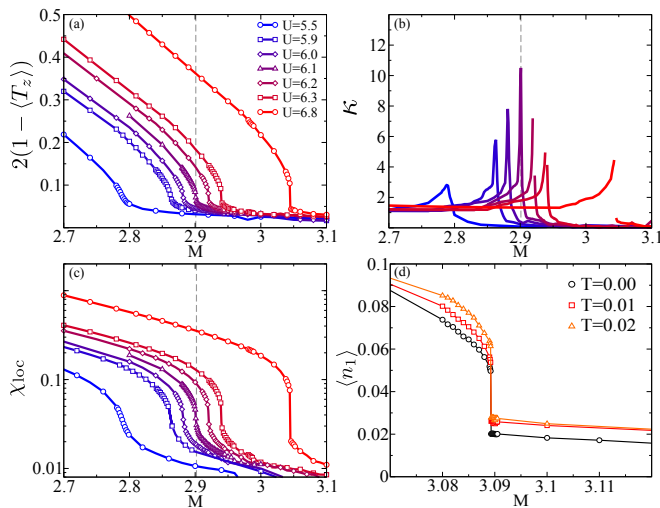


Figure 3. Observable signatures of the topological quantum phase transition in the strongly correlated regime. The four panels shows examples of different experimentally measurable quantities as a function of the mass term M , potentially useful to characterise the transition to a QSHI in presence of interaction. (a) Local orbital polarisation $2(1 - \langle T_z \rangle)$. (b) Orbital compressibility $\kappa = -2\partial\langle T_z \rangle/\partial M$ (c) Local spin susceptibility at $\omega=0$. (d) Temperature dependence of the jump in the orbital occupation of the first (higher-lying) orbital.

similarly to $\langle T_z \rangle$ as a function of M and U . Remarkably, as demonstrated in Fig. 3(c), this characteristic behaviour shows up also in χ_{loc} , i.e. in a true physical response function.

Finally, we give evidence that the discontinuity at the topological phase transition for $U > U_c$ is not only visible at zero but also at finite temperatures. As shown in Fig. 3(d), the orbital occupation (only the higher-lying orbital is shown) changes slightly because of temperature broadening effects, but the jump remains visible. As long as T does not overcome the size of the gap, which in our case is set by the strength of the orbital hybridisation λ , we hence expect the discontinuity and the critical behaviour of the bulk observables discussed here to be detectable.

DISCUSSION

We have given robust numerical evidence that, in the presence of strong electronic correlations, the topological phase transition from a trivial BI to a QSHI becomes an actual thermodynamic transition. In particular, the zero temperature phase diagram of Fig. 1(a) in the $1/M-1/U$ plane is remarkably similar to the $P-T$ phase diagram for a liquid-phase transition. The analogy between the two diagrams can be pushed even further: both feature indeed also a third phase, a Mott insulator for our model

and a solid state in the diagram of a simple fluid (e.g. CO_2) as well as a triple point.

The immediate consequence of this thermodynamic character of the topological transition is the presence of a well-defined critical behaviour of simple bulk quantities such as the orbital compressibility and the local spin susceptibility, as we have discussed in detailed in the previous section. A more imaginative idea inspired by this analogy with the thermodynamics of the liquid-gas transition, is a – hitherto unforeseen – strategy to design a correlation-induced QSHI: Instead of looking for the right bulk material with d - or f -electrons, one could think of a mechanism to increase “by hand” the correlation strength in a BI. This may be achieved by building a heterostructure of a Mott insulator and a non-inverted, i.e., trivial BI. This way, the BI layers close to the interface with the Mott insulator will get a negative contribution to the mass term by “proximity effect” [45]. If this is done in the region of the first order line (i.e. “at low enough temperatures”, which according to our analogy correspond to high enough values of U), the distinction between the liquid and the gas phases would be thermodynamically well-defined, unlike what happens in the super-critical (uncorrelated) region where the two states are not thermodynamically distinct.

ACKNOWLEDGEMENTS

We thank F. Assaad, M. Fabrizio, M. Punk and A. Toschi for useful discussions. A.A. and M.C. are supported by the European Union under FP7 ERC Starting Grant n.240524 “SUPERBAD”. G.S. acknowledges financial support from the DFG research units FOR1162 and FOR1346, J.C.B. from the ERC Synergy Grant “UQUAM” and B.T. from the DFG-JST research unit “Topotronics”, the DFG priority program SPP1666, the Helmholtz Foundation (VITI) and the ENB graduate school on “Topological Insulators”.

-
- [1] M. Z. Hasan and C. L. Kane, Rev. Mod. Phys **82**, 3045 (2010).
 - [2] J. E. Moore, Nature **464**, 194 (2010).
 - [3] X.-L. Qi and S.-C. Zhang, Rev. Mod. Phys **83**, 1057 (2011).
 - [4] C. L. Kane and E. J. Mele, Phys. Rev. Lett. **95**, 226801 (2005).
 - [5] C. L. Kane and E. J. Mele, Phys. Rev. Lett. **95**, 146802 (2005).
 - [6] B. A. Bernevig, T. L. Hughes, and S.-C. Zhang, Science **314**, 1757 (2006).
 - [7] M. König *et al.*, Science **318**, 766 (2007).
 - [8] A. P. Schnyder, R. S. A. Furusaki, and A. W. W. Ludwig, Phys. Rev. B **78**, 195125 (2008).
 - [9] A. Kitaev, AIP Conf. Proc. **1134**, 226801 (2009).

- [10] S. Ryu, A. P. Schnyder, F. A., and A. W. W. Ludwig, *New. J. Phys.* **12**, 065010, (2010).
- [11] A. Altland and M. R. Zirnbauer, *Phys. Rev. B* **55**, 1142 (1997).
- [12] K. v. Klitzing, D. G., and P. M., *Phys. Rev. Lett.* **45**, 494 (1980).
- [13] R. B. Laughlin, *Phys. Rev. B* **23**, 5632 (1981).
- [14] D. J. Thouless, M. Kohmoto, M. P. Nightingale, and M. den Nijs, *Phys. Rev. Lett.* **49**, 405 (1982).
- [15] S. Raghu, X.-L. Qi, C. Honerkamp, and S.-C. Zhang, *Phys. Rev. Lett.* **100**, 156401 (2008).
- [16] D. Pesin and L. Balents, *Nature Phys.* **6**, 376 (2010).
- [17] L. A. Wray *et al.*, *Nature Phys.* **76**, 32 (2010).
- [18] D. Xiao, W. Zhu, Y. Ran, N. Nagaosa, and S. Okamoto, *Nature Commun.* **2**, 596 (2011).
- [19] A. Rüegg and G. A. Fiete, *Phys. Rev. Lett.* **108**, 046401 (2012).
- [20] M. Hohenadler and F. F. Assaad, *J. Phys.: Condens. Matter* **25**, 143201 (2013).
- [21] M. Kargarian and G. A. Fiete, *Phys. Rev. Lett.* **110**, 156403 (2013).
- [22] X. Deng, K. Haule, and G. Kotliar, *Phys. Rev. Lett.* **111**, 176404 (2013).
- [23] I. F. Herbut and L. Janssen, *Phys. Rev. Lett.* **113**, 106401 (2014).
- [24] F. F. Assaad and I. F. Herbut, *Phys. Rev. X* **314**, 031010 (2013).
- [25] J. C. Budich, B. Trauzettel, and G. Sangiovanni, *Phys. Rev. B* **87**, 235104 (2013).
- [26] A. Georges, L. de' Medici, and J. Mravlje, *Annu. Rev. Condens. Matter Phys.* **45**, 137 (2013).
- [27] A. Georges, G. Kotliar, W. Krauth, and M. J. Rozenberg, *Rev. Mod. Phys* **68**, 13 (1996).
- [28] J. C. Budich, R. Thomale, G. Li, M. Laubach, and S.-C. Zhang, *Phys. Rev. B* **86**, 201407(R) (2012).
- [29] N. Parragh *et al.*, *Phys. Rev. B* **88**, 195116 (2013).
- [30] A. I. Lichtenstein and M. I. Katsnelson, *Phys. Rev. B* **57**, 6884 (1998).
- [31] G. Kotliar *et al.*, *Rev. Mod. Phys* **78**, 865 (2006).
- [32] K. Held, *Adv. Phys.* **56**, 829 (2007).
- [33] Z. Wang, X.-L. Qi, and S.-C. Zhang, *Phys. Rev. B* **85**, 165126 (2012).
- [34] Z. Wang and S.-C. Zhang, *Phys. Rev. X* **2**, 031008 (2012).
- [35] P. Werner and A. J. Millis, *Phys. Rev. Lett.* **99**, 126405 (2007).
- [36] M. Sentef, J. Kuneš, P. Werner, and A. P. Kampf, *Phys. Rev. B* **80**, 155116 (2009).
- [37] S. Rachel and K. Le Hur, *Phys. Rev. B* **82**, 075106 (2010).
- [38] M. Ezawa, Y. Tanaka, and N. Nagaosa, *Sci. Rep.* **3**, 2790 (2013).
- [39] J. C. Budich, *Phys. Rev. B* **87**, 161103(R) (2013).
- [40] V. Gurarie, *Phys. Rev. B* **83**, 085426, (2011).
- [41] M. Wu *et al.*, *Phys. Rev. B* **88**, 125124 (2013).
- [42] E. Benckiser *et al.*, *Nature Mater.* **10**, 189 (2011).
- [43] C. H. Pennington and V. A. Stenger, *Rev. Mod. Phys* **68**, 855 (1996).
- [44] F. Anfuso and S. Eggert, *Phys. Rev. Lett.* **96**, 017204 (2006).
- [45] G. Borghi, M. Fabrizio, and E. Tosatti, *Phys. Rev. B* **81**, 115134 (2009).